



# Ultraslow phonon-assisted collapse of tubular image states

Dvira Segal \*, Petr Král, Moshe Shapiro

*Department of Chemical Physics, Weizmann Institute of Science, 76100 Rehovot, Israel*  
*Department of Chemistry and Physics, The University of British Columbia, Vancouver V6T1Z1, Canada*

Received 17 August 2004; accepted for publication 5 January 2005

Available online 13 January 2005

## Abstract

We predict ultraslow collapse of “tubular image states” (TIS) on material surfaces. TIS are bound Rydberg-like electronic states formed at large distances ( $\sim 30$  nm) from the surfaces of suspended circularly-symmetric nanowires, such as metallic C nanotubes. The states are formed in potential wells, resulting from a combination of the TIS-electron attraction to image charges in the nanotube and its centrifugal repulsion, caused by spinning around the tube. We demonstrate that TIS can collapse on the tube surface by passing their angular momentum  $l$  to circularly polarized flexural phonons excited in the tube. Our analysis shows that for highly detached TIS with  $l \geq 6$  the relaxation lifetimes are of the order of 10 ns–1  $\mu$ s, while for  $l < 6$  these lifetimes are reduced by several orders of magnitude.

© 2005 Elsevier B.V. All rights reserved.

**Keywords:** Many-body and quasi-particle theories; Surface electronic phenomena (work function, surface potential, surface previous termstates, etc.); Phonons

## 1. Introduction

Electronic image states formed above flat metallic surfaces [1] could be very attractive for various potential applications, if their lifetimes were not too short (typically of the order of a few ps), due to their overlap with the surface states [2]. Therefore, we have suggested to study electronic image

states in the vicinity (but far above) of suspended linear conductors, such as metallic carbon nanotubes. The formed “tubular image states” (TIS) [3–5] are expected to be much more stable, by being highly detached from their surfaces [3], as a result of the interplay between the attraction of the TIS-electron to its image charge in the nanotube and the centrifugal repulsion, due to its circular motion about the cylinder.

These unique states can be characterized by the continuous linear momentum  $k$ , describing motion along the tube axis, and the discrete  $(n, l)$  radial and angular momentum numbers. Typically, TIS

\* Corresponding author. Address: Department of Chemical Physics, Weizmann Institute of Science, 76100 Rehovot, Israel. Tel.: +1 972 8 9342012; fax: +1 972 8 9344123.

E-mail address: [dvira.segal@weizmann.ac.il](mailto:dvira.segal@weizmann.ac.il) (D. Segal).

with the angular momentum  $l \geq 6$  are separated 10–50 nm away from the surface, and their energies are a few meV below the vacuum level. In recent experiments [6], TIS with low  $l < 3$  were observed to form in the vicinity of suspended nanotubes. Their lifetimes are about one order of magnitude longer than image states above flat metallic surfaces, in agreement with our expectations.

In this work, we analyze in details the process of the TIS-electron collapse on the surface of the nanotube. This process is controlled by the relaxation of the TIS angular momentum  $l$ , and described by the lifetime  $\tau_l$ . In highly detached TIS, the relaxation can be very slow, since their angular momentum is only weakly coupled to elementary excitations in the nanotube. Such a behavior is analogous to the relaxation of spins in materials, controlled by the weak spin–orbital coupling [7,8]. In general, TIS-electron can be relaxed radiatively or via collisions with nanotube’s electrons or phonons. From these, only the last seem to be crucial in the TIS-collapse: the radiative transitions are too weak in the meV regime, and the scattering on the tube electrons mainly causes changes in the TIS linear momentum  $k$  [9–11]. In contrast, the coupling of the TIS-electron to the nanotube’s phonons can, in addition to relaxing the linear momentum  $k$  [12], relax the TIS-electron spinning, that is, its angular momenta  $l$ , and its radial motion, that is, its principal quantum number  $n$ .

## 2. Coupling of the TIS-electron to nanotube phonons

Nanotubes can perform rich type of motions, such as “piston-like” oscillations [13], “centrifuge-like” ultrafast rotations [14] or various internal vibrations [15]. Out of these, those that can carry angular momentum should be of potential interest for damping of the TIS. The most relevant seems to be “string-like” vibrations associated with circularly polarized flexural phonon modes [16–18], schematically shown in Fig. 1.

We first derive the Hamiltonian for the coupling of the TIS-electron to these phonon modes. We consider an electron placed at a distance  $\rho$  from

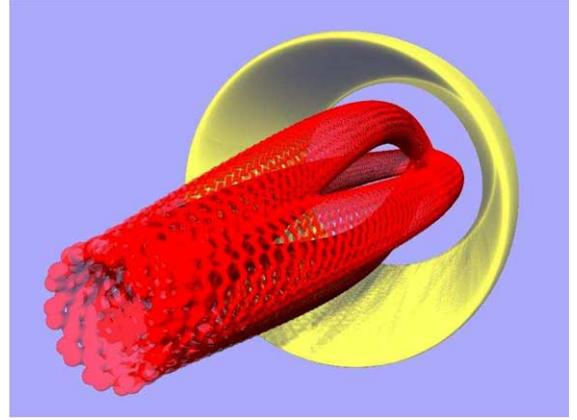


Fig. 1. The flexural deformation of a nanotube excited by the spinning TIS-electron.

the center of an ideally conducting, infinitely long, cylinder of radius  $a$  [3,19]. The electron is electrostatically attracted to the image charge induced on the surface of the cylinder by a potential of the approximate form,

$$V(\rho) \approx \frac{2e^2}{\pi a} \sum_{n=1,3,5,\dots} \text{li}[(a/\rho)^n],$$

$$\text{where } \text{li}(x) \equiv \int_0^x \frac{dt}{\ln(t)}. \quad (1)$$

This potential interpolates well between the far-from-the-surface  $-\frac{e^2}{\rho \ln(\rho/a)}$  and near-to-the-surface  $\frac{1}{|\rho-a|}$  forms. Adding the repulsive centrifugal potential, we get an effective potential,

$$V_{\text{eff}}(\rho) = V(\rho) + \frac{\hbar^2(l^2 - \frac{1}{4})}{2m_e \rho^2}, \quad (2)$$

where  $m_e$  is the electron mass. The wave functions, associated with the TIS-electron motion in this potential, are separable in the cylindrical coordinates,

$$\Psi_{n,l,k}(\rho, \varphi, z) = \psi_{n,l}(\rho) e^{il\varphi} \phi_k(z) / \sqrt{2\pi\rho}, \quad (3)$$

where  $\phi_k(z) = e^{ikz} / \sqrt{\mathcal{L}}$  and  $\mathcal{L}$  is a normalization length in the longitudinal  $z$  direction. The corresponding eigenenergies are  $E_{n,l,k} = E_{n,l} + E_k$ , where  $E_{n,l}$  is related with the radial electronic motion, and  $E_k = \frac{\hbar^2 k^2}{2m_e}$  is the kinetic energy for the longitudinal motion along the wire. The radial wave functions  $\psi_{n,l}(\rho)$  satisfy the Schrödinger equation,

$$\left(-\frac{\hbar^2}{2m_e} \frac{d^2}{d\rho^2} + V_{\text{eff}}(\rho) - E_{n,l}\right) \psi_{n,l}(\rho) = 0. \quad (4)$$

The wave functions with high  $l > 5$  turn out to be highly detached from the surface, due to the presence of the centrifugal barrier, so the TIS-electron hardly sees the detailed atomic structure of the surface. It thus only feels the tube like a polarizable elastic string that vibrates in a direction perpendicular to the axis, as depicted in Fig. 1. For a (10, 10) carbon nanotube this type of motion is characterized either by a linear [15,20] or by a quadratic dispersion relation  $\omega_q = v_p a q^2$ , where  $v_p \approx 15$  km/s is a phonon velocity and  $a = 0.68$  nm is the tube radius [17,18]. In the present problem, the exact character of the dispersion is less relevant, as it leads to very similar relaxation times.

The force exerted by the radially directed vibrations of the nanotube on the TIS-electron is derived from the change in the tube's equilibrium position, which in turn changes the effective potential  $V_{\text{eff}}(\rho, z)$ . For simplicity, we use the screening potential in the approximate Coulombic form,  $1/|\rho - a|$ . Hence, when the nanotube, oriented along the  $z$  axis, is displaced by the vector  $\vec{\delta}(z) = (\delta_x(z), \delta_y(z))$  from its equilibrium position  $\vec{\rho}_0 = (x_0, y_0)$ , the potential energy can be written as,

$$V(\rho, z) = \frac{-e^2}{4 \left[ (x_e - x_0 + \delta_x(z))^2 + (y_e - y_0 + \delta_y(z))^2 \right]^{1/2} - a}, \quad (5)$$

where  $(x_e, y_e, z_e)$  is the external electron position, with  $\rho = \sqrt{x_e^2 + y_e^2}$ . In order to evaluate the effective electron–phonon coupling Hamiltonian, we expand the potential function of Eq. (5) in a Taylor series about the equilibrium position

$$V(\rho, z) = V(\rho)|_{\vec{\delta}=0} + \vec{\delta}(z) \cdot \nabla V(\rho)|_{\vec{\delta}=0} + \frac{1}{2} (\vec{\delta}(z) \cdot \nabla) (\vec{\delta}(z) \cdot \nabla) V(\rho)|_{\vec{\delta}=0} + \dots, \quad (6)$$

and keep only the first order contribution. Then the total Hamiltonian of the system can be written as,

$$H = \frac{-\hbar^2}{2m_e} \nabla^2 + V(\rho)|_{\vec{\delta}=0} + H_{\text{ph}} + \vec{\delta}(z) \cdot \nabla V(\rho)|_{\vec{\delta}=0}, \quad (7)$$

where the first two terms describe the TIS-electron energy for a rigid tube,  $H_{\text{ph}}$  is the free-phonon Hamiltonian and the last term describes the effective electron–phonon coupling  $H_{\text{e-ph}}$  [21].

The tube's displacement  $\vec{\delta}(z) = \hat{x}\delta_x(z) + \hat{y}\delta_y(z)$  can be expanded in the normal-mode coordinates  $u_{k,\mu}$  ( $\mu = x, y$ ),

$$\vec{\delta}(z) = \sum_q (\hat{x}u_{q,x} + \hat{y}u_{q,y}) e^{iqz}, \quad (8)$$

where  $q$  are the phonon wave vectors. Defining the circular polarization complex directions  $\hat{\epsilon}_{\pm} \equiv \hat{x} \pm i\hat{y}$ , the tube's displacement can be written as  $\vec{\delta}(z) = \hat{\epsilon}_+ \delta_+(z) + \hat{\epsilon}_- \delta_-(z)$ , where  $\delta_{\pm}(z) = (\delta_x(z) \mp i\delta_y(z))/2$ . Using these variables, we can convert Eq. (8) to an expansion in circularly polarized phonon modes that can carry angular momentum,

$$\vec{\delta}(z) = \sum_q (u_{q,+} \hat{\epsilon}_+ + u_{q,-} \hat{\epsilon}_-) e^{iqz}; \quad (9)$$

$$u_{q,\pm} = (u_{q,x} \mp iu_{q,y})/2.$$

The  $x, y$  partial derivatives of the potential energy are (omitting the  $-e^2/4$  factor)

$$\frac{\partial V}{\partial x} \Big|_{\vec{\delta}=0} = \frac{\cos \varphi}{(\rho - a)^2}, \quad \frac{\partial V}{\partial y} \Big|_{\vec{\delta}=0} = \frac{\sin \varphi}{(\rho - a)^2}, \quad (10)$$

or in terms of the circular polarization variables,

$$\partial_{\pm} V \equiv \frac{\partial V}{\partial \epsilon_{\pm}} \Big|_{\vec{\delta}=0} = \frac{e^{\pm i\varphi}}{(\rho - a)^2}, \quad (11)$$

$$\varphi = \tan^{-1} \left( \frac{y_e - y_0}{x_e - x_0} \right).$$

Next, we evaluate the first order coupling elements between the  $\Psi_v(\rho, \varphi, z)$  ( $v = (n, l, k)$ ) and  $\Psi_{v'}(\rho, \varphi, z)$  electronic states of Eq. (3), given in terms of the overlap integrals,

$$I_{\pm} = \int \Psi_v^* (\delta_{\pm} \partial_{\pm} V) \Psi_{v'} \rho \, d\rho \, d\varphi \, dz$$

$$= \frac{1}{2\pi \mathcal{L}} \sum_q u_{q,\pm} \int e^{i(l'-l)\varphi} e^{\pm i\varphi} \, d\varphi \int e^{i(k'-k)z} e^{iqz} \, dz$$

$$\times \int \psi_{n,l}^*(\rho) \frac{-e^2}{4(\rho - a)^2} \psi_{n',l'}(\rho) \, d\rho$$

$$= \sum_q u_{q,\pm} A_{q,\pm}^{(v,v')}. \quad (12)$$

The  $z$  and  $\varphi$  integrations yield  $\delta(k' - k + q)$  and  $\delta(l' - l \pm 1)$ , respectively, which gives the longitudinal and angular momentum conservation. The  $A_{q,\pm}^{(v,v')}$  terms denote the coupling elements for the  $(n, l, k) \rightarrow (n', l', k')$  transitions, induced by the right and left circularly polarized phonons, respectively, with longitudinal momentum  $q$ .

We can now quantize the normal-mode coordinates and write them in terms of the  $a_q^\dagger$  and  $a_q$  phonon creation and annihilation operators,

$$u_{q,\pm} = \sqrt{\frac{\hbar}{4MN\omega_q}} (a_{q,\pm}^\dagger + a_{q,\pm});$$

$$a_{q,\pm} = (a_{q,x} \pm ia_{q,y})/\sqrt{2}, \quad (13)$$

where  $M$  is the mass of a carbon atom and  $N$  denotes the number of unit cells along the tube. Defining the new coupling elements as  $\tilde{A}_{q,\pm}^{(v,v')} = \sqrt{\frac{\hbar}{4MN\omega_q}} A_{q,\pm}^{(v,v')}$ , we can write the free-phonon Hamiltonian and the electron–phonon interaction Hamiltonian as,

$$H_{\text{ph}} = \sum_{q,\pm} \hbar\omega_q a_{q,\pm}^\dagger a_{q,\pm},$$

$$H_{\text{e-ph}} = \sum_{q,\pm,v,v'} \tilde{A}_{q,\pm}^{(v,v')} (a_{q,\pm}^\dagger + a_{q,\pm}) c_v^\dagger c_{v'}. \quad (14)$$

Here,  $c_v^\dagger$  and  $c_v$  are the creation and annihilation operators, respectively, of TIS-electrons in the  $\psi_v(\rho)$  states. In addition to the linear momentum  $k' = k - q$ , and angular momentum  $l' = l \pm 1$ , conservation rules, the Hamiltonian (14) yields the energy conservation condition,

$$\frac{\hbar^2 k^2}{2m_e} + E_{n,l} = \frac{\hbar^2 k'^2}{2m_e} + E_{n',l'} \pm \hbar\omega_q. \quad (15)$$

Using the quadratic phonon dispersion relation  $\omega_q = v_p a q^2$ , denoting  $\Delta E = E_{n,l} - E_{n',l'}$ , and substituting  $k' = k - q$ , we obtain a quadratic equation for  $q$

$$\left( \frac{\hbar^2}{2m_e} \pm \hbar v_p a \right) q^2 - \frac{\hbar^2}{m_e} k q - \Delta E = 0. \quad (16)$$

From Eq. (16), we obtain all the solutions for the phonon momentum  $q$ , which correspond to the emission and absorption processes, where the electron and phonon can propagate in different directions. Note that for an electron initially at rest,  $k = 0$ , we have that  $q \propto \sqrt{\Delta E}$ .

### 3. Numerical results and discussion

We evaluate the  $A_{q,\pm}^{(v,v')}$  coupling matrix elements for different transitions associated with the (10, 10) carbon nanotube of the radius  $a = 0.7$  nm. In Fig. 2 (left), we show these matrix elements for the  $v = (n = 10, l) \rightarrow v' = (n', l - 1)$  transitions, with  $l = 7-9$ . As expected, the elements are larger for small  $l$ , for which the electron is localized closer to the tube surface and can more easily excite the phonons. In addition, as  $n'$  decreases, the small  $l$  coupling elements increase faster, relative to the large  $l$  terms. This behavior is due to the fast collapse on the surface of the small  $l$ , small  $n$ , electronic wave functions. Note also that the strongest

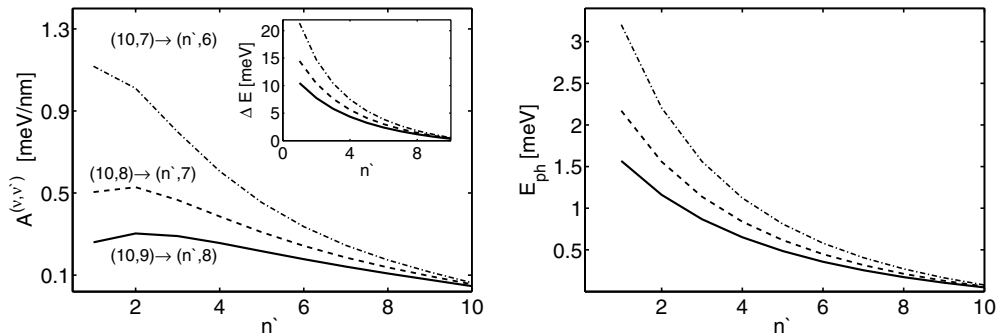


Fig. 2. (Left) Electron–phonon coupling elements for the  $(10, l) \rightarrow (n', l - 1)$  relaxations processes. Full line:  $l = 9$ ; dashed:  $l = 8$ ; dashed-dotted:  $l = 7$ . The inset shows the corresponding energy differences  $\Delta E$  for these transitions. (Right) Excited phonon energies  $E_{\text{ph}}$  for the same processes shown on the left.

coupling occurs for transitions to the  $n' = 1, 2$  states, which experience the strongest screening potential.

In the right panel of Fig. 2, we display the energies of phonons,  $E_{\text{ph}} \equiv \hbar\omega_q$ , excited by the processes shown in the left panel of this figure. These energies are computed for a phonon velocity of  $v_p = 15$  km/s and an electron that is initially at rest, that is,  $k = 0$ . We see that the phonon energies are proportional to  $\Delta E$  and tend to rapidly fall with  $n'$ . We find that most of the electronic radial energy is funneled to the electronic longitudinal kinetic energy, and only  $\sim 10\%$  is given to the phonons.

We now use the above coupling elements to evaluate the relaxation rates  $v = (n, l, k) \rightarrow v' = (n', l', k')$ , at  $T = 0$  K, by using the Fermi's golden rule [22],

$$\begin{aligned} W_{v \rightarrow v'} &= \frac{2\pi}{\hbar} \left| \tilde{A}_{q,\pm}^{(v,v')} \right|^2 \delta(E_k + \Delta E - E_{k'} - \hbar\omega_q) \\ &= \frac{2\pi}{\hbar} \left( \frac{\hbar}{4MN\omega_q} \right) |f|^2 \delta_{l-l', \pm 1} \delta_{k-k', q} \\ &\quad \times \delta(E_k + \Delta E - E_{k'} - \hbar\omega_q). \end{aligned} \quad (17)$$

In the last expression,  $f$  accounts for the radial part of the overlap integral in Eq. (12). Summing over all the final electronic continuum  $k'$  states, leads to

$$\begin{aligned} W_{(n,l,k) \rightarrow (n',l')} &= \sum_{k'} W_{v \rightarrow v'} \\ &= \frac{\mathcal{L}}{\hbar} |f|^2 \delta_{l-l', \pm 1} \\ &\quad \times \sum_{k'} \left( \frac{\hbar}{4MN\omega_{k-k'}} \right) \frac{1}{|dE_{k'}/dk'|}, \end{aligned} \quad (18)$$

where the sum involves only the  $k'$  values that fulfill the energy and momentum conservation requirements. The free-electron dispersion is  $dE_k/dk = \hbar^2 k/m_e$ , and  $\mathcal{L}/N = 2.49$  Å for the (10, 10) nanotube, where  $\mathcal{L}$  is the tube length and  $N$  the number of elementary cells.

The computed relaxation rates  $W_{v \rightarrow v'}$  can be used to evaluate the angular momentum lifetime  $\tau_l$ , which determines the collapse of the TIS-electron on the surface of the tube. We define  $\tau_l$  via the relation,

$$\langle L(t) \rangle = L_0 e^{-t/\tau_l}, \quad (19)$$

where  $L(t) = \sum_v \hbar l c_v^\dagger(t) c_v(t)$ , ( $v = (n, l, k)$ ) is the angular momentum operator in the Heisenberg representation. Then, we can calculate  $\tau_l$  from the second order expansion of the Heisenberg equation of motion for the expectation value of  $\dot{L}(t)$ ,

$$\begin{aligned} \langle \dot{L}(t) \rangle &= -\frac{1}{\hbar^2} \int_0^t d\tau \langle [H(t), [H(\tau), L(\tau)]] \rangle \\ &= -\sum_{v'} \hbar(l-l') W_{v \rightarrow v'}, \end{aligned} \quad (20)$$

where  $H(t)$  is the system Hamiltonian. Combining Eqs. (19) and (20), yields  $\tau_l$  of the  $(n, l = L_0/\hbar, k)$  state

$$\tau_l^{-1} = \sum_{v'} (1 - l'/l) W_{v \rightarrow v'}, \quad \tau_v^{-1} = \sum_{v'} W_{v \rightarrow v'}. \quad (21)$$

Here, we also show the dephasing lifetime  $\tau_v$  describing relaxation of the  $v$  state. These two relaxation times can be measured in different experimental setups. It is clear from Eq. (21) that  $\tau_l \rightarrow \infty$ , when the  $l \rightarrow l \pm 1$  up and down transition rates are comparable. This situation can occur when the electron longitudinal momentum is high enough such that  $\hbar^2 k^2/2m_e \gg \Delta E$ . If the  $l \rightarrow l + 1$  process is absent, we obtain that  $\tau_l = l\tau_v$ . This  $\tau_l$  can still be very long, in analogy to forward scattering processes [12], since states with large initial  $l$  can only be relaxed in many scattering events.

In Fig. 3, we display the calculated  $\tau_l$  for different initial states  $v = (n, l, k)$ . As expected, states with large angular momenta, highly detached from the surface (see left inset), have very long  $\tau_l \approx 10$ –500 ns (left panel). On the other hand, states with  $l \sim 1$ –4 that are separated only  $\sim 1$  nm from the surface have much shorter lifetimes. The effect of the proximity to the surface, causes the low  $l$  couplings to be 2–3 orders of magnitude stronger than the high  $l$  couplings, leading to a 4–6 orders of magnitude increase in the low  $l$  angular momentum relaxation rates. This picture is consistent with the right panel of Fig. 3, where we show that the lifetimes go up as we increase  $n$ , thereby further removing the TIS-electron from the surface. The  $\tau_l$  lifetimes also get longer for high  $l$  values when the initial  $k$  is increased, allowing for excitation

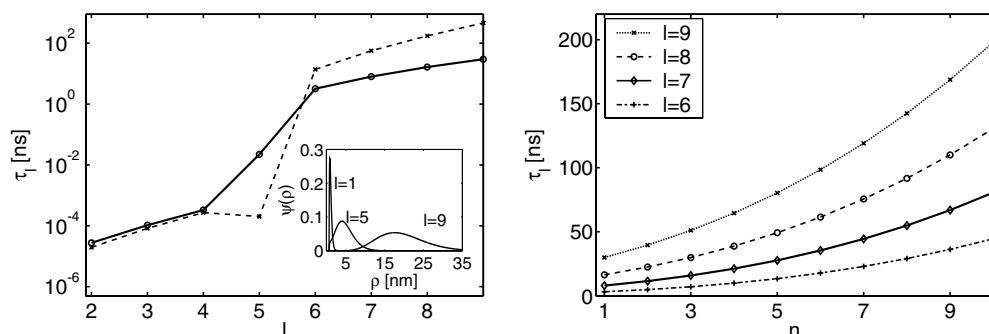


Fig. 3. Angular relaxation time for the  $(n, l, k)$  state at  $T = 0$  K. (Left):  $n = 1, k = 0$  (full);  $n = 1, k = 10^9 \text{ m}^{-1}$  (dashed). The inset shows the  $n = 1$  radial states for the  $l = 1, 5, 9$  cases. (Right): The  $n$ -dependence of  $\tau_l$  for  $l = 6-9$ .

processes with  $l \rightarrow l + 1$  for  $\Delta E < 0$ . The accuracy of the above calculations for low  $l$  is not as high as for high  $l$ , because our wave functions do not represent the states accurately enough close to the surface. In this region, coupling to other phonon modes becomes relevant [17], and additional effects play a role [23]. The accuracy is also limited by the simplified Coulomb form used for the screening potential.

At finite temperatures we need to consider the emission/absorption processes induced by thermal phonons. The associated atomic vibration amplitudes in Eq. (13) are given by  $\lambda_q = \left[ \frac{\hbar(n_q + \frac{1}{2} \pm \frac{1}{2})}{4MN\omega_q} \right]^{1/2}$ , where  $n_q = (e^{\hbar\omega_q/k_B T} - 1)^{-1}$ ,  $k_B$  is the Boltzmann constant and the plus (minus) sign is for emission (absorption) processes. At room temperatures and for the  $l \sim 7-9$  detached states, we find from Fig. 2 that  $k_B T / \hbar\omega_q \sim 5-50$ . Hence, the transition rates increase relative to the  $T = 0$  case by the same factor. In an analogous fashion, we can evaluate the two-phonon emission rates, but their values are expected to be much smaller. The ultraslow TIS lifetimes can be tuned by changing the conductivity [4] and tension in the nanotubes (stretching), which might lead to interesting novel applications.

### Acknowledgments

We acknowledge numerous useful discussions with H.R. Sadeghpour and B.E. Granger. This project was supported by a grant from the Feinberg graduate school of the WIS.

### References

- [1] N.D. Lang, W. Kohn, Phys. Rev. B 7 (1973) 3541.
- [2] U. Höfer, I.L. Shumay, Ch. Reuß, U. Thomann, W. Wallauer, Th. Fauster, Science 277 (1997) 1480.
- [3] B.E. Granger, P. Král, H.R. Sadeghpour, M. Shapiro, Phys. Rev. Lett., 89 (2002) 135506–1.
- [4] D. Segal, P. Král, M. Shapiro, Phys. Rev. B 69 (2004) 153405.
- [5] D. Segal, B.E. Granger, H.R. Sadeghpour, P. Král, M. Shapiro, Phys. Rev. Lett. 94 (2005) 016402; D. Segal, P. Král, M. Shapiro, Chem. Phys. Lett. 392 (2004) 314.
- [6] M. Zamkov et al., Phys. Rev. Lett. 93 (2004) 156803; M. Zamkov et al., Phys. Rev. B 70 (2004) 115419.
- [7] J.M. Kikkawa, I.P. Smorchkova, N. Samarth, D.D. Awschalom, Science 277 (1997) 1284; J.M. Kikkawa, D.D. Awschalom, Phys. Rev. Lett. 80 (1998) 4313.
- [8] R. Hanson, B. Witkamp, L.M.K. Vandersypen, L.H. Willems van Beveren, J.M. Elzerman, L.P. Kouwenhoven, Phys. Rev. Lett. 91 (2003) 196802.
- [9] T. Pichler, M. Knupfer, M.S. Golden, J. Fink, A. Rinzler, R.E. Smalley, Phys. Rev. Lett. 80 (1998) 4729.
- [10] T. Stöckli, J.M. Bonard, A. Châtelain, Z.L. Wang, P. Stadelmann, Phys. Rev. B, 64 (2001) 115424–1.
- [11] N. Zabala, E. Ogando, A. Rivacoba, F.J. Garcia de Abajo, Phys. Rev. B, 64 (2001) 205410–1; A. Rivacoba, F.J. Garcia de Abajo, Phys. Rev. B 67 (2003) 085414.
- [12] P. Král, Phys. Rev. B 53 (1996) 11034.
- [13] Q. Zheng, Q. Jiang, Phys. Rev. Lett. 88 (2002) 045503.
- [14] P. Král, H.R. Sadeghpour, Phys. Rev. B 65 (2002) 161401(R).
- [15] M.S. Dresselhaus, G. Dresselhaus, Ph. Avouris, Synthesis, Structure, Properties and Applications, Springer-Verlag, 2001.
- [16] R. Gao, Z.L. Wang, Z. Bai, W.A. de Heer, L. Dai, M. Gao, Phys. Rev. Lett. 85 (2000) 622.
- [17] H. Suzuura, T. Ando, Phys. Rev. B 65 (2002) 235412.

- [18] G.D. Mahan, Phys. Rev. B 65 (2002) 235402;  
G.D. Mahan, G.S. Jeon, Phys. Rev. B 70 (2004) 075405.
- [19] J.C. Slater, N.H. Frank, Electromagnetism, McGraw-Hill, NY, 1947.
- [20] R. Saito, T. Takeya, T. Kimura, G. Dresselhaus, M.S. Dresselhaus, Phys. Rev. B 57 (1998) 4145.
- [21] G.D. Mahan, Many Particle Physics, Plenum Press, New York, 1993.
- [22] J. Jiang, R. Saito, A. Grüneis, G. Dresselhaus, M.S. Dresselhaus, Chem. Phys. Lett. 392 (2004) 383.
- [23] Z. Qian, V. Sahni, Phys. Rev. B 66 (2002) 205103.